Proceedings of ICRC 2001: 1271 © Copernicus Gesellschaft 2001

ICRC 2001

Modeling of electromagnetic showers in ice at $E \sim 1$ TeV

S. Razzaque[1], **S. Seunarine**[3], **D. Z. Besson**[1], **D. W. McKay**[1], **D. Seckel**[2], **and J. Adams**[3]

[1]The University of Kansas, Lawrence, KS 66045, U.S.A
[3]The University Of Canterbury, Private Bag 4800, Christchurch, New Zealand
[2]Bartol Research Institute, The University of Delaware, Newark, DE 19716, U.S.A

Abstract. We use a *GEANT* based Monte Carlo simulation to investigate the properties of electron induced electromagnetic showers in ice. Various shower parameters such as *critical energy*, *Moliere radius*, and *track lengths* are studied. We look at the dependence of these quantities on the energy of the primary electron as well as the Monte Carlo threshold energy. We also study in detail the Cerenkov radiation associated with the charge excess in the shower. The radiation is coherent at frequencies on the order of GHz and can readily be detected by experiments such as the RICE at the South Pole.

1 Introduction

Ultra High Energy neutrinos interacting in a dense medium such as ice produce electrons with very high energy. A single high energy electron can initiate a cascade of photons, electrons, and positrons in the ice through bremsstrahlung and pair production, the two process that are dominant at high energies(Rossi, 1952). As a cascade develops and the particles reach a *critical energy*, E_c, other processes such as continuous energy loss, Moller, Bhabha, and Compton scattering become important. Continuous energy loss (due to atomic excitation or ionization) degrades the energy of the charged particles which results in the termination of the shower. Moller, Bhabha, and Compton scattering eject atomic electrons into the shower resulting in the build up of an excess negative charge. Positron annihilation also contributes to the negative *charge excess*.

The shower particles travel faster than the speed of light in the medium and therefore emit (broadband) Cerenkov radiation. The Cerenkov *pulse* that is observed will be the coherent superposition of the signals from all tracks when the dimension of the excess charge region is smaller than the radiated wavelength and both are small compared to the distance to the observer, as discussed in Section 4. The transverse size of the shower, caused by multiple scattering, is characterized by the *Moliere radius*, R_m, roughly 13 cm for ice. This is the dimension to which coherence is sensitive, and the corresponding frequencies are of order GHz. Since the observation distances are typically hundreds of meters, the conditions for coherence are satisfied. At high enough energy, the large number of coherently radiating charges more than compensate for the low frequency suppression of the Cerenkov pulse from radio relative to optical. The feasibility of detecting this signal is discussed by Frichter, G. et al, 1995.

Correspondence to: D. Z. Besson (dbesson@ku.edu)

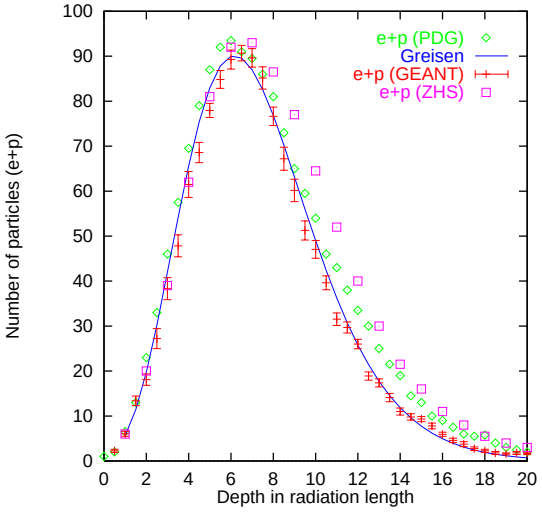

Fig. 1. The longitudinal profile in iron of 30 GeV *GEANT* showers, and showers produced by *EGS4*, and *ZHS*. The solid line is the fit of a Greisen distribution to the data.

2 Monte Carlo Details

GEANT is a widely used Monte Carlo package that can simulate elementary particle physics processes and detectors. This latter facility allows one to define unique detector materials. For our study we defined our detector medium to be a cube of ice (H_2O of density .92 g/cm^3). We ensured that

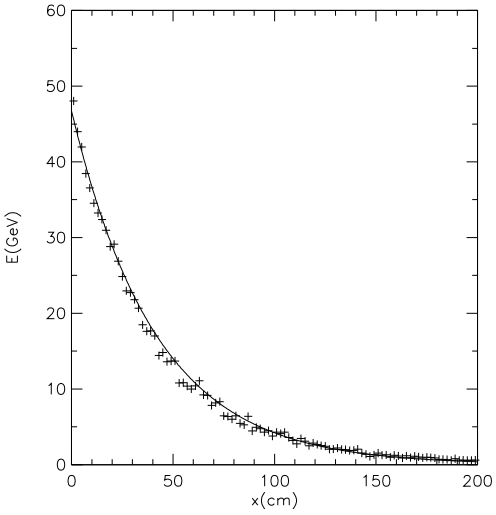

Fig. 2. Average energy, in ice, of 500 50 GeV electrons vs distance in cm. Crosses indicate Monte Carlo data points and the solid line is the exponential fit. This fit gives a radiation length of 42 cm. A 0.611 MeV kinetic energy threshold was used in all 500 simulations.

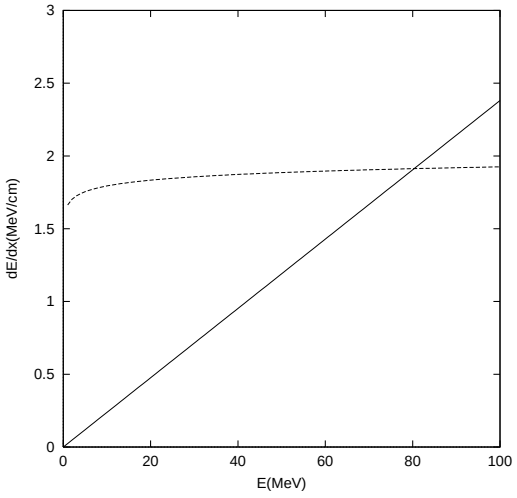

Fig. 3. Critical energy determined by the crossing of $\frac{dE}{dx}_{ionization}$(curve) and $\frac{dE}{dx}_{bremsstrahlung}$(straight line). The straight line is obtained from $dE/dx = -E/x_0$ and using the radiation length obtained from Fig.2. The low energy rise in the ionization loss curve is not shown on this scale.

the size of the cube was big enough so that all particles in the highest energy showers studied were contained within the cube. Particles are transported (*tracked*) taking into account physical processes due to the particles themselves and due to the tracking medium. Cross sections for various interactions are calculated by *GEANT* using the density, atomic number, and mass number of the detector material. The Monte Carlo threshold energy, E_{th}, is used by *GEANT* to calculate total cross sections. E_{th} also determines the minimum energy at which particles are tracked.

In our configuration of *GEANT* we initiate electromagnetic showers with single high energy electrons. We keep track of all particles in the shower, e^-, e^+, and γ, above E_{th}. For each track in a shower we store information about its start and end position, the start time of the track, the energy at the start position, and any continuous energy loss between start and end points. For a high energy electron, for example, information about radiated photons, continuous loss and any δ-production can be written out at all interaction points along its trajectory. From this detailed track information, we calculate the electromagnetic pulse emitted by the shower. We will not consider the nuclear recoil in the neutrino interaction which will produce a hadronic shower.

3 Results

3.1 Longitudinal Profile

To check that we were using the *GEANT* code correctly we ran the simulation with iron as the detector material. This allowed us to compare the showers we obtained with those of other Monte Carlo programs. Fig. 1 shows a comparison of the longitudinal profile of 30 GeV showers in iron obtained from *GEANT*, the *EGS4* code system(from Groom and Klein, 2000), and the *ZHS* Monte Carlo(Zas et al., 1992). Also shown is a Greisen distribution fit to the data(Rossi and Greisen, 1941).

3.2 Energy Loss

The radiation length, x_o, of a material is defined as the average distance over which an electron loses all but $1/e$ of its energy due to bremsstrahlung. This can be calculated by tracking energy loss due to bremsstrahlung and fitting an exponential, $< E >= E_o e^{-x/x_o}$, to the data. Fig. 2 shows an exponential fitted to the energy loss data for 50 GeV electrons. From the fit we obtain a radiation length of 42 cm.

The exponential growth of the number of shower particles stops when the average particle energy drops below the critical energy, E_c, the energy at which ionization losses become important. There are two definitions of E_c. Energy loss of an electron due to radiation is given by the Bethe-Heitler formula(Heitler, 1954). The Bethe-Bloch formula gives the energy loss due to ionization. One definition of E_c is the energy at which both of these losses are equal. The other definition of critical energy, the so-called Rossi definition, is the energy at which the ionization loss per radiation length is equal to the particle's energy. Fig. 3 shows the crossing curves for bremsstrahlung and ionization loss. From these we get a critical energy of 81 MeV. E_c obtained from the Rossi definition will be $5-7\%$ smaller than this(Groom and Klein, 2000).

3.3 Lateral Spread

Multiple scattering is responsible for the lateral spread of the shower. The transverse(to the shower axis) size of the shower is described by the Moliere radius, R_M. It is determined by

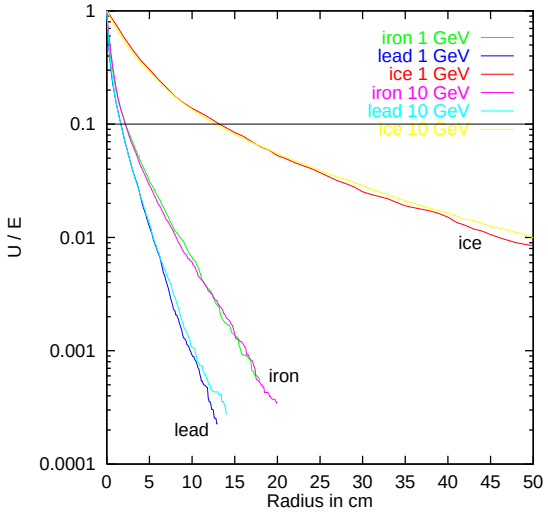

Fig. 4. Plotted is U/E. U is the energy flow across a cylinder of radius r cm, integrated over the evolution of the shower. Curves are shown for ice, carbon and iron at two different energies. The horizontal is drawn at $U/E = 10\%$ from which we directly read off R_M. As expected the plots show that R_M in independent of energy

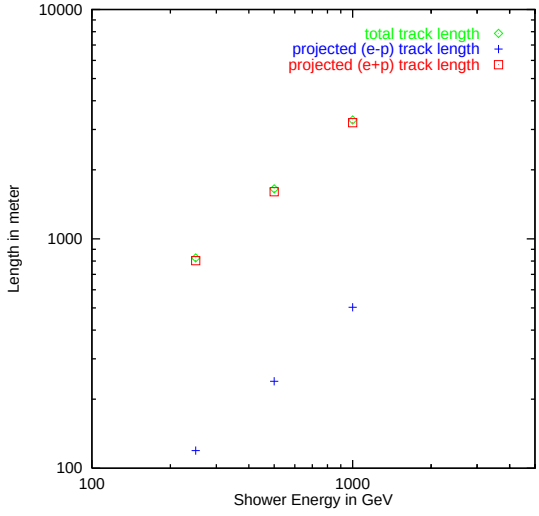

Fig. 5. Track lengths as functions of shower energy for *GEANT* simulations. Shown are total($e^- + e^+$) track length, total track length projected along the shower axis, and total excess($e^- - e^+$) projected track length. Track lengths scale linearly with the shower energy, as does the electric field pulse from the shower at the Cherenkov angle. All total energy thresholds are set at $1.51\ MeV$.

the average angular deflection per radiation length at E_c due to multiple Coulomb scattering. About 90% of the energy transported in the shower is contained within a "cylinder" of radius $1\ R_M$ centered on the shower axis(Rossi, 1952).

The Moliere radius is related to the E_c and x_o of the material through the equation, $R_M = (x_o\ 21\text{MeV})/E_c$. E_c appearing here is that obtained from the Rossi definition. Notice that R_M is independent of energy. We can calculate R_M from *GEANT* track information by looking at the transverse energy flow in the shower and estimating the radial distance within which 90% of the energy is contained. This is the energy integrated over the evolution of the shower(Nelson et al., 1966). In the Monte Carlo calculation a cylinder of infinite length is used. Fig. 4 shows the results for ice, lead and iron. The Moliere radii for these are 13 cm, 1.6 cm, and 2.1cm respectively.

3.4 Track Length and $\frac{dE}{dx}$

The strength of the Cerenkov pulse depends on the tracklength of the excess negative charge. Ionization caused by charged particles travelling through matter is usually described in terms of energy loss as a function of distance, $\frac{dE}{dx}$. If all the processes except ionization are elastic, then the total tracklength can be estimated from $E_0/\frac{dE}{dx}$. For ice dE/dx in the relativistic rise region is of order 1.8 MeV/cm. In all cases the estimate of tracklengths obtained using this value agree with those measured from shower data. Fig. 5 shows how the tracklength changes with primary electron energy. It shows the expected linear scaling of tracklength with primary energy.

4 Radio Pulses from Electromagnetic Showers

For a single charged particle moving in a dense medium starting at some point r_1 and traveling for time δt with speed $\boldsymbol{v}$, the electric field, $\boldsymbol{E}$, observed at some *far* distance, R, is given by Eqn. 1. $n = \sqrt{\epsilon\mu}$ is the refractive index of the medium, $\boldsymbol{\beta} = \frac{\boldsymbol{v}}{\boldsymbol{c}}$, and $\hat{\boldsymbol{n}}$ is a unit vector from the shower track to the observer. The expression is valid: (1) at distances large compared to the size of the particle's track where $\hat{\boldsymbol{n}}$ can be approximated by a constant vector for the entire trajectory of the particle; (2) when $ka^2/R << 1$, so the high order terms in the phase can be neglected, where a is the length of the particle's track. This is the *Fraunhoffer* limit(Zas et al., 1992).

$$R\boldsymbol{E}(\omega) = \frac{\mu_r}{\sqrt{2\pi}}\left(\frac{e}{c^2}\right) e^{i\omega\frac{R}{c}} e^{i\omega(t_1 - n\boldsymbol{\beta}\cdot\boldsymbol{r}_1)} \times \boldsymbol{v}_T \frac{(e^{i\omega\delta t y(1-\hat{n}\cdot\boldsymbol{\beta}n)} - 1)}{1 - \hat{n}\cdot\boldsymbol{\beta}n}, \quad (1)$$

where $\boldsymbol{v}_T = \hat{\boldsymbol{n}} \times (\hat{\boldsymbol{n}} \times \boldsymbol{v})$. The particle velocity $\boldsymbol{v}$ in the medium can be greater than that of light. The condition $1 - \hat{n}\cdot\boldsymbol{\beta}n = 0$ defines the Cherenkov angle θ_c as $\cos\theta_c = 1/n\beta$. At or very close to the Cherenkov angle, Eqn. 1 reduces to the form,

$$R\boldsymbol{E}(\omega) = \frac{\mu_r i\omega}{\sqrt{2\pi}}\left(\frac{e}{c^2}\right) e^{i\omega\frac{R}{c}} e^{i\omega(t_1 - n\boldsymbol{\beta}\cdot\boldsymbol{r}_1)} \boldsymbol{v}_T \delta t. \quad (2)$$

The term $\boldsymbol{v}_T\delta t$ is the projection of the track length vector perpendicular to the observation direction, $\hat{\boldsymbol{n}}$, which shows explicitly the origin of the dependence of pulse height on the tracklength. In the Monte Carlo, Eqn. 2 is used near and at the Cerenkov angle for numerical stability because there

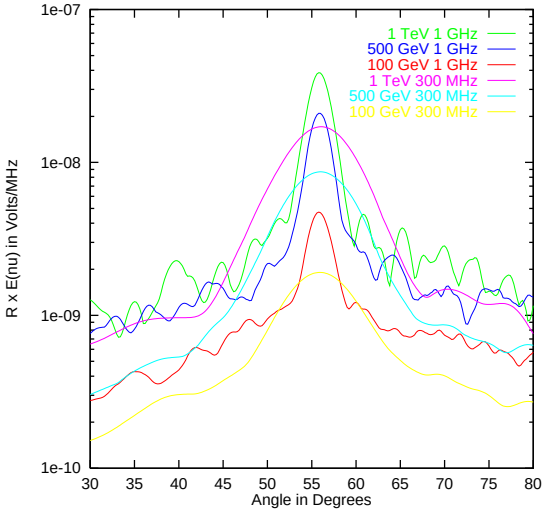

Fig. 6. Angular distribution of electric field, using Eqns. 1 and 2, from electromagnetic showers in ice with energies 1TeV, 500GeV and 100GeV at 1GHz and 300MHz frequencies. Each curve is the averaged of 20 showers with total energy threshold $E_{th} = 1.511\mathrm{MeV}$.

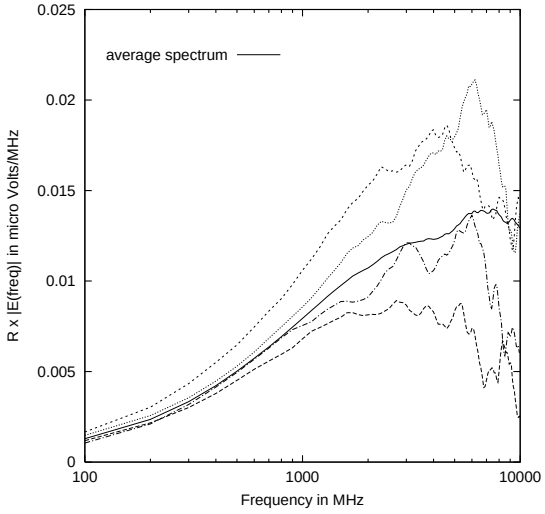

Fig. 7. Frequency spectrum at the Cherenkov angle for 100GeV showers with 100 KeV kinetic E_{th}. The solid line is the average spectrum of 30 showers and the dashed lines are 4 spectrums from individual showers.

the denominator in Eqn. 1 becomes zero. The electric field due to a shower is the vector sum of the fields due to each track. Far away from the shower, where Eqn. 1 is valid, the shower can be treated as a single extended radiating charge (the charge being the charge excess). The principle radiating region is at shower maximum, where the average energy is E_c and the width is of order 1m in ice.

4.1 Electric Field

To calculate the electric field from a shower we summed the contributions from all charged tracks. We can assume azimuthal symmetry about the shower axis long as we have many tracks in the shower (a typical 500GeV shower has thousands of tracks). This allows us to evaluate the pulse equations on a plane through the shower axis. We checked this *2D* approximation explicitly on a shower by shower basis and did not find any noticeable difference between the pulses evaluated in the $x-z$ plane and in the $y-z$ plane. In Fig. 6, we show the pulses from 1 TeV, 500 GeV and 100 GeV showers at 1 GHz and 300 MHz frequencies using the *2D* approximation. All pulses are averaged over 20 showers and a total E_{th} of 1.511 MeV. The Cerenkov angle is at $\approx 55.8^o$ as expected from the refractive index of ice, $n = 1.78$. From studies of the Cerenkov pulse we found that the peak of the pulse at θ_c scales linearly with energy. We also observed at θ_c that the Gaussian half width is inversely proportional to the frequency which is analogous to a slit diffraction pattern. Both of these properties are somewhat discernible in Fig. 6

4.2 Frequency Spectrum

In Fig. 7 we show the frequency spectrum of the Cerenkov signal. For this plot we did not restrict the calculation to a plane. We calculated the field using the full three dimensional geometry of the shower. We see that the coherence is maintained up to a few GHz. Beyond this frequency range(i.e. at shorter wavelengths) coherence breaks down as the radiated wavelengths approach the dimensions of the emitting region.[1] The signal in the coherent regime can be detected by dipole receivers such as the ones deployed by the RICE experiment (Seckel, D., et al., 2001).

Acknowledgements. We thank Jaime Alvarez-Muniz for many useful discussions and working sessions which were crucial to our understanding of the ZHS code. We thank George Frichter, John Ralston, and Roman Buniy for helpful suggestions. We thank Florian Hardt for work done early in the project. We thank Tim Bolton for assisting with the initial setup of *GEANT*. This work is supported in part by NSF, DOE, University of Kansas GRF, University of Canterbury Marsden Grant, and the facilities of the Kansas Institute of Theoretical and Computational Science.

References

Rossi, B., High Energy Particles, Prentice Hall, 1952
Frichter, G. M. et al., Phys. Rev. D53:1684, 1996
Groom, D. E. and Klein, S., R., Passage of Particles Through Matter, in Review of Particle Physics, Eur. Phys. J. C15:163, 2000
Zas, E. et al., Phys. Rev. D45:362, 1992
Rossi, B. and Greisen, K., Revs. Mod. Phys., 13:240, 1941
Heitler, W., The Quantum Theory of Radiation, Clarendon, 1954
Nelson, W. R. et al., Phys. Rev. 149:201, 1966
Seckel, D. et al., 2001, these proceedings.

[1] The results obtained with *GEANT* differ from the results of Zas et al., 1992. A detailed description of our study and explanations of the differences between the *GEANT* and *ZHS* Monte Carlos will be given elsewhere(Razzaque, S. et al. in preparation)